A Comparison of Salient and Nonsalient Pole Line-Start Permanent Magnet Synchronous Machines

J. M. Lee
Dept. of Electrical and Computer Engineering
1415 Engineering Drive
Madison, WI 53706

***Abstract* – Saliency affects the starting performance of line-start permanent magnet synchronous machines (LS-PMSM). Some of these effects, including differences in torque, speed, and synchronization time characteristics, are detailed in this paper. Additionally, specific attention was given to the performance of LS-PMSM right before synchronization – a period of time when this type of machine "pulls-in" to the synchronous speed.**

I. Introduction

Line-start permanent magnet synchronous machines (LS-PMSMs) have many advantages over other machine designs. A LS-PMSM can achieve a higher efficiency and higher power factor than high-efficiency induction motor designs. The permanent magnet costs of this machine, although high, can be recovered through the energy savings gained by using this type of motor [3]. The LS-PMSM designs studied in this paper include a starting cage that is necessary to asynchronously start the machine. This cage is very similar to the rotor cage used in an induction machine. When a LS-PMSM is instantaneously connected to an excitation source, a torque is created by the cage, which is also called the 'cage torque.' The torque produced by the rotor permanent magnets ('magnet torque') opposes the cage torque because it acts as a braking torque. The cage torque must be large enough to accomplish two tasks: 1) overcome the magnet torque in order to rotate the rotor, and 2) spin the rotor fast enough to obtain synchronism. In addition to these rotor cage details, the saliency of the machine can provide additional insights into the starting performance of the LS-PMSM. In this paper, salient and nonsalient cases of the LS-PMSM were compared to more deeply understand asynchronous characteristics. First, the ac machine equations for the LS-PMSM were derived to provide the basis for the simulations. Second, the modeling parameters and methodology are discussed. Lastly, results and conclusions of this modeling are presented.

II. Derivation of LS-PMSM Equations

The defining equations for the line-start permanent magnet synchronous machine were formed in order to conduct simulations. Using Park's Equations, constraints were made with regard to the LS-PMSM [1]. First, the rotor reference frame was used throughout this analysis in order to be in the same reference frame as the permanent magnets, which appears as a constant value in this reference frame. Second, a flux linkage for the permanent magnet λ_{pm} was defined. This flux linkage appears in the d-axis of the stator (s) and rotor (k) flux linkage. Park's Equations in this constrained form for the LS-PMSM are described in (1)-(8).

$$v_{ds} = r_s \cdot i_{ds} + p \cdot \lambda_{ds} - \omega_r \cdot \lambda_{qs} \quad (1)$$

$$v_{qs} = r_s \cdot i_{qs} + p \cdot \lambda_{qs} + \omega_r \cdot \lambda_{ds} \quad (2)$$

$$0 = r_{kd} \cdot i_{kd} + p \cdot \lambda_{kd} \quad (3)$$

$$0 = r_{kq} \cdot i_{kq} + p \cdot \lambda_{kq} \quad (4)$$

where

$$\lambda_{ds} = L_{ls} \cdot i_{ds} + L_{md}(i_{ds} + i_{kd}) + \lambda_{pm} \quad (5)$$

$$\lambda_{qs} = L_{ls} \cdot i_{qs} + L_{mq}(i_{qs} + i_{kq}) \quad (6)$$

$$\lambda_{kd} = L_{lkd} \cdot i_{kd} + L_{md}(i_{kd} + i_{ds}) + \lambda_{pm} \quad (7)$$

$$\lambda_{kq} = L_{lkq} \cdot i_{kq} + L_{mq}(i_{kq} + i_{qs}) \quad (8)$$

For the simulations, the flux voltage formulations of the ac machine equations were desired. Multiplying (5)-(8) by the base angular frequency gives (9)-(12).

$$\psi_{ds} = X_{ls} \cdot i_{ds} + \psi_{md} + \psi_{pm} \quad (9)$$

$$\psi_{qs} = X_{ls} \cdot i_{qs} + \psi_{mq} \quad (10)$$

$$\psi_{kd} = X_{lkd} \cdot i_{kd} + \psi_{md} + \psi_{pm} \quad (11)$$

$$\psi_{kq} = X_{lkq} \cdot i_{kq} + \psi_{mq} \quad (12)$$

where

$$\psi_{md} = X_{md} \cdot (i_{ds} + i_{kd}) \quad (13)$$

$$\psi_{mq} = X_{mq} \cdot (i_{qs} + i_{kq}) \quad (14)$$

Then, the stator and rotor currents were found by manipulating (9)-(12). The currents are given in (15)-(18).

$$i_{ds} = \frac{\psi_{ds} - \psi_{md} - \psi_{pm}}{X_{ls}} \quad (15)$$

$$i_{qs} = \frac{\psi_{qs} - \psi_{mq}}{X_{ls}} \quad (16)$$

$$i_{kd} = \frac{\psi_{kd} - \psi_{md} - \psi_{pm}}{X_{lkd}} \quad (17)$$

$$i_{kq} = \frac{\psi_{kq} - \psi_{mq}}{X_{lkq}} \quad (18)$$

These currents are then placed into (13) and (14) in order to solve for a magnetizing d- and q-axis flux voltage

completely in terms of other flux voltages. These are shown in (19) and (22), where the reactance definitions of (20), (21), and (23) help to simplify (19) and (22).

$$\psi_{md} = \left(\frac{X_{md}^{*}}{X_{ls}}\right)\cdot\psi_{ds} + \left(\frac{X_{md}^{*}}{X_{lkd}}\right)\cdot\psi_{kd} - \left(\frac{X_{md}^{*}}{X_{md}^{**}}\right)\cdot\psi_{pm} \tag{19}$$

where

$$X_{md}^{*} = \frac{1}{\frac{1}{X_{md}} + \frac{1}{X_{ls}} + \frac{1}{X_{lkd}}} \tag{20}$$

$$X_{md}^{**} = \frac{1}{\frac{1}{X_{ls}} + \frac{1}{X_{lkd}}} \tag{21}$$

$$\psi_{mq} = \left(\frac{X_{mq}^{*}}{X_{ls}}\right)\cdot\psi_{qs} + \left(\frac{X_{mq}^{*}}{X_{lkq}}\right)\cdot\psi_{kq} \tag{22}$$

where

$$X_{mq}^{*} = \frac{1}{\frac{1}{X_{mq}} + \frac{1}{X_{ls}} + \frac{1}{X_{lkq}}} \tag{23}$$

With (15)-(18) and (9)-(12), (1)-(4) can now be completely expressed by flux voltages as (24)-(27) show.

$$v_{ds} = \frac{r_s}{X_{ls}}\cdot\left(\psi_{ds} - \psi_{md} - \psi_{pm}\right) + \frac{p}{\omega_B}\cdot\psi_{ds} - \frac{\omega_r}{\omega_B}\cdot\psi_{qs} \tag{24}$$

$$v_{qs} = \frac{r_s}{X_{ls}}\cdot\left(\psi_{qs} - \psi_{mq}\right) + \frac{p}{\omega_B}\cdot\psi_{qs} + \frac{\omega_r}{\omega_B}\cdot\psi_{ds} \tag{25}$$

$$0 = \frac{r_{kd}}{X_{lkd}}\cdot\left(\psi_{kd} - \psi_{md} - \psi_{pm}\right) + \frac{p}{\omega_B}\cdot\psi_{kd} \tag{26}$$

$$0 = \frac{r_{kq}}{X_{lkq}}\cdot\left(\psi_{kq} - \psi_{mq}\right) + \frac{p}{\omega_B}\cdot\psi_{kq} \tag{27}$$

Rearranging (24)-(27) and solving for the stator and rotor flux voltages results in (28)-(31), which are very useful for modeling the LS-PMSM using simulation software.

$$\psi_{ds} = \left(\frac{1}{p}\right)\left(\omega_B\right)\left[v_{ds} - \frac{r_s}{X_{ls}}\cdot\left(\psi_{ds} - \psi_{md} - \psi_{pm}\right) + \frac{\omega_r}{\omega_B}\cdot\psi_{qs}\right] \tag{28}$$

$$\psi_{qs} = \left(\frac{1}{p}\right)\left(\omega_B\right)\left[v_{qs} - \frac{r_s}{X_{ls}}\cdot\left(\psi_{qs} - \psi_{mq}\right) - \frac{\omega_r}{\omega_B}\cdot\psi_{ds}\right] \tag{29}$$

$$\psi_{kd} = \left(\frac{1}{p}\right)\left(\omega_B\right)\left[\frac{-r_{kd}}{X_{lkd}}\cdot\left(\psi_{kd} - \psi_{md} - \psi_{pm}\right)\right] \tag{30}$$

$$\psi_{kq} = \left(\frac{1}{p}\right)\left(\omega_B\right)\left[\frac{-r_{kq}}{X_{lkq}}\cdot\left(\psi_{kq} - \psi_{mq}\right)\right] \tag{31}$$

In addition to the electrical ac machine equations for the LS-PMSM, the mechanical equation given by (32) was used to model basic torque dynamics of the rotor.

$$\omega_r = \left(\frac{1}{p}\right)\left(\frac{\omega_B}{M}\right)\left(T_e - T_L\right) \tag{32}$$

III. Modeling Two Cases

Two cases were modeled during the simulation of the LS-PMSM: salient and nonsalient. A nonsalient pole machine has two constraints: 1) $X_{ds} = X_{qs}$ and 2) $X_{md} = X_{mq}$. These two constrains are not equal for a salient pole machine. The parameter values for the salient pole LS-PMSM are given in Table 1 [1].

TABLE 1
Parameters of the Simulated LS-PMSM

Quantity	Value	Per Unit V [pu]
Power (Base)	3730 W (5 hp)	1
Voltage (l-l RMS)	230 V	-
Voltage (l-n Peak) (Base)	187.8 V	1
Frequency (f)	60 Hz	-
Angular Freq. (ω_s) (Base)	377 rad/sec	1
Poles	2	-
r_s	0.32 Ω	0.0226
r_kd	0.99 Ω	0.0698
r_kq	2 Ω	0.141
L_md	23 mH	0.611
L_mq	50 mH	1.329
L_ds	26.2 mH	0.697
L_qs	53.2 mH	1.415
L_kd	29.4 mH	0.781
L_kq	56.4 mH	1.5
J	0.01 Nm-s^2	-

For the salient pole machine, the per-unit values of X_{ds}, X_{qs}, X_{md}, X_{mq}, and saliency ratio are given in (33)-(37) at ω_s = 1pu.

$$X_{ds} = 0.697 \tag{33}$$

$$X_{qs} = 1.415 \tag{34}$$

$$X_{md} = 0.611 \tag{35}$$

$$X_{mq} = 1.329 \tag{36}$$

$$Saliency\_Ratio \equiv \frac{X_{ds}}{X_{qs}} \cong 0.4926 \tag{37}$$

For the nonsalient pole machine, the per-unit values of X_{ds}, X_{qs}, X_{md}, and X_{mq} are given in (38)-(39) at ω_s = 1pu.

$$X_{ds} = X_{qs} = 0.697 \tag{38}$$

$$X_{md} = X_{mq} = 0.611 \tag{39}$$

The goal of modeling these two cases is to compare starting characteristics of the LS-PMSM, and come to conclusions about how saliency affects asynchronous starting performance. These simulations were conducted under no-load conditions. After the simulation results, a summary of

the steady state values for both nonsalient and salient LS-PMSMs has been given in Table 2. These steady state results provide an additional layer of insight into the effects of saliency on these types of machines.

IV. Salient & Nonsalient LS-PMSM Machines

Simulation results below place salient and nonsalient pole results in contrast with each other, highlighting the differences between the two.

Fig. 1 and 2 show the speed vs. torque plots of a nonsalient (Fig. 1) and salient (Fig. 2) pole machine. These two figures show the instantaneous torque of the machine, which is composed of both average and pulsating torque components [2].

For the nonsalient pole machine, the cage torque provides the average torque needed for asynchronous starting, and is the only component of average torque. The pulsations in the instantaneous torque are present due to the magnets, which induce oscillations in the torque [3]. Because this machine is nonsalient, there is no difference in the q- and d-axis reactance. This symmetry results in the absence of an additional torque component – the reluctance torque. In contrast, the salient pole machine, by definition and in reality, contains a difference in these reactance components, resulting in a reluctance torque that assists in the synchronizing process.

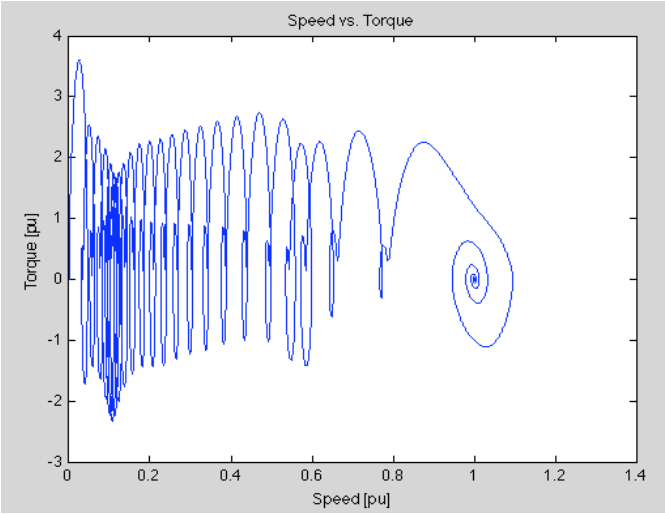

Fig. 1. Instantaneous torque dynamics of the nonsalient pole LS-PMSM.

With this additional torque component, the salient pole machine has a greater inherent ability to overcome the magnet torque, which provides a braking torque at all speeds [3]. The magnet torque's oscillations are still present, but its frequency is reduced. Also, as the right-most portion of Fig. 2 displays, the pull-in characteristics are far less oscillatory, and much quicker. These better dynamics are a result of the additional reluctance torque and saliency.

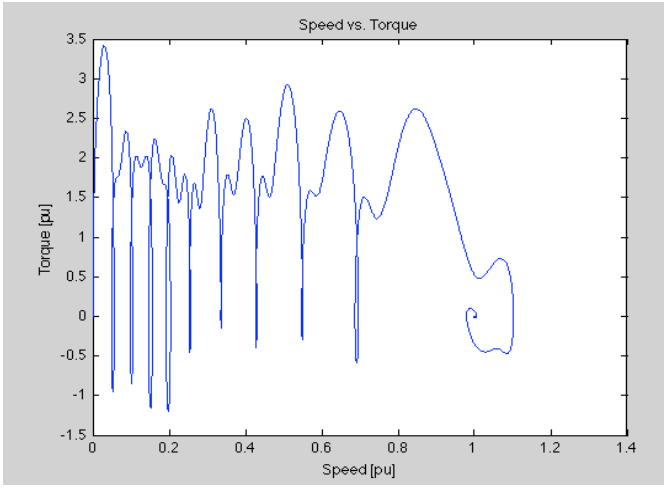

Fig. 2. Instantaneous torque dynamics of the salient pole LS-PMSM.

The salient pole LS-PMSM can pull into synchronism faster than the nonsalient pole machine. This difference is specifically due to the additional reluctance torque, adding more average torque to overcome the braking torque of the magnets.

Fig. 3 shows the nonsalient rotor speed during asynchronous starting conditions. Synchronization is complete around 1.25 seconds. In contrast, as Fig. 4 shows, synchronization for the salient pole machine is complete around 0.75 seconds. The pulsations from the magnet torque are present in both figures, although they are larger and more frequency for the nonsalient pole machine.

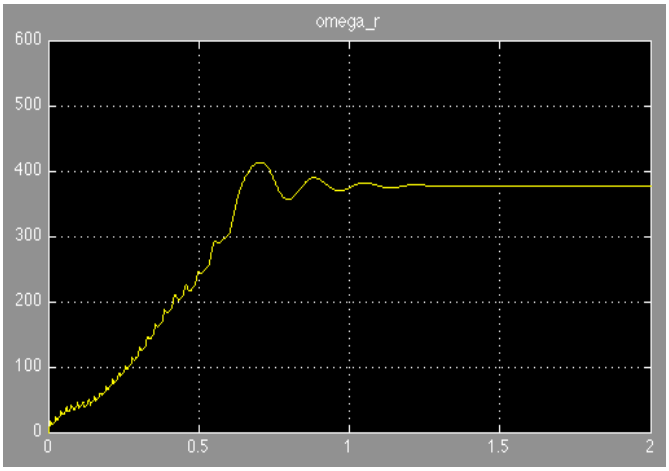

Fig. 3. Nonsalient pole rotor speed [rad/sec] during start-up time [sec].

Analysis of the torque angle was also conducted. In the simulation, the torque angle was defined at the integral of the slip frequency. Equation (40) shows this relation.

$$\delta = \frac{1}{p}\left(\omega_e - \omega_r\right) \qquad (40)$$

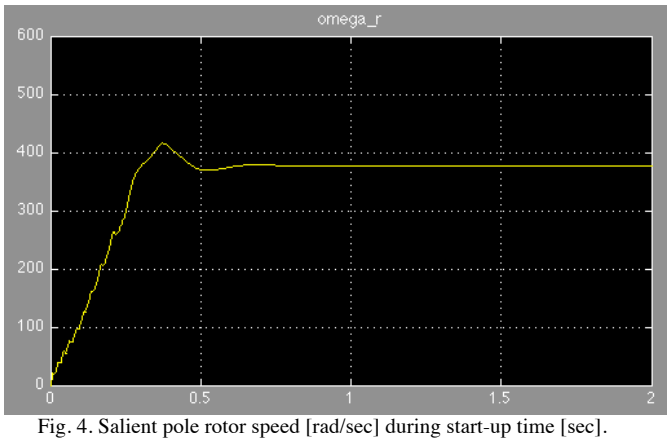

Fig. 4. Salient pole rotor speed [rad/sec] during start-up time [sec].

The torque angle was plotted against the slip in both of the cases under study. Because the machine is starting from standstill, the slip begins at 1 pu.

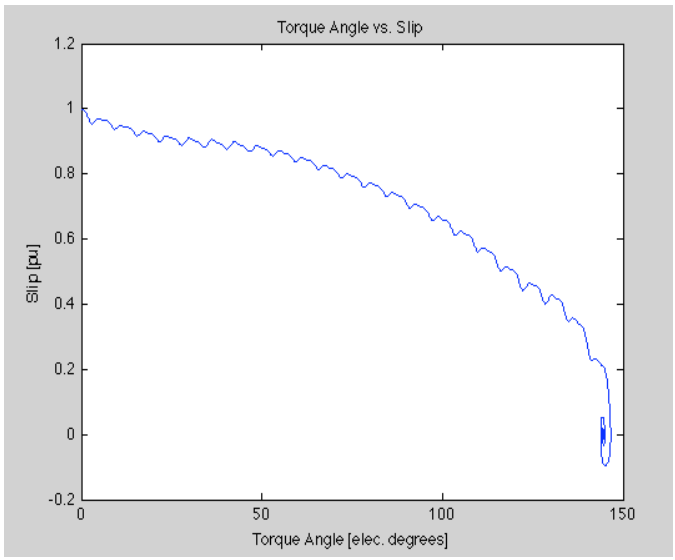

Fig. 5. Nonsalient δ-slip characteristic.

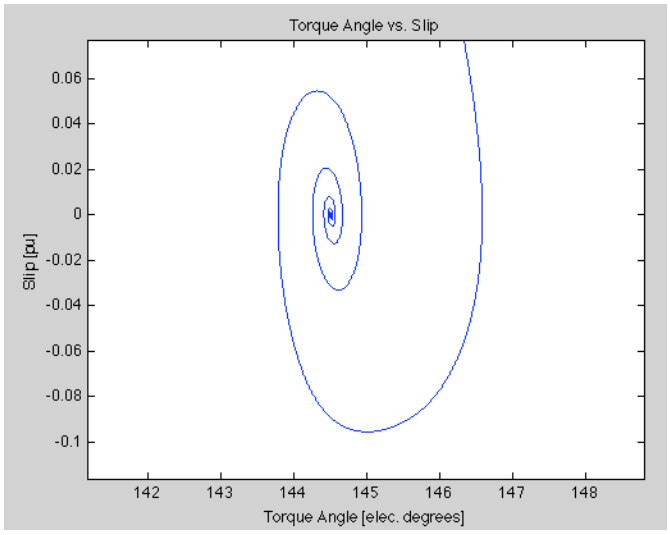

Fig. 6. Inset of pull-in details of Fig. 5.

Figs. 5 and 6 show the nonsalient case. Here the torque angle extends from zero to just under 145 electrical degrees. Fig. 6 details the pull-in of the nonsalient machine. Without the reluctance torque, only the cage torque (generated through line excitation) is left to bring the machine into synchronism, and a large torque angle is needed to generate a sufficient amount of cage torque.

Figs. 7 and 8 detail the salient-pole case's torque angle vs. slip (δ-slip) relationship. Due to the additional reluctance torque, a smaller torque angle is needed because a lower cage torque value will now be able to bring the machine to synchronization. Here, the torque angle, starting from standstill, ends at just over 56 electrical degrees. Fig. 8 details the pull-in of the salient pole machine. Again, fewer oscillations around the synchronous point occur before total synchronization is achieved. For emphasis, the torque angle vs. instantaneous torque results are also given on the next page of this report (Figs. 9-12).

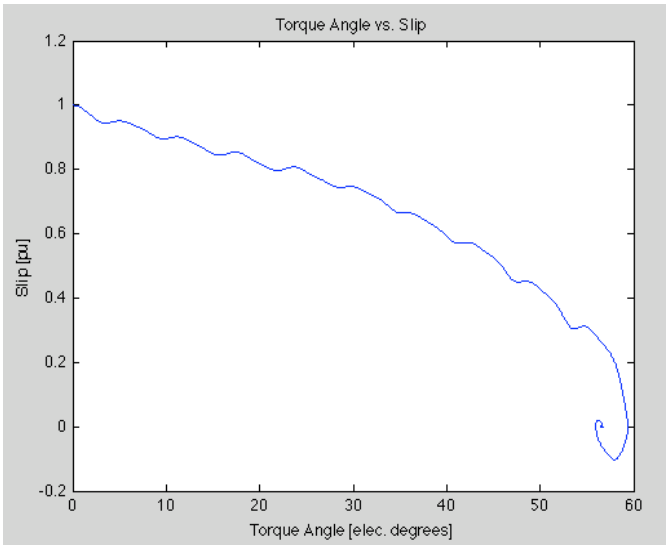

Fig. 7. Salient δ-slip characteristic.

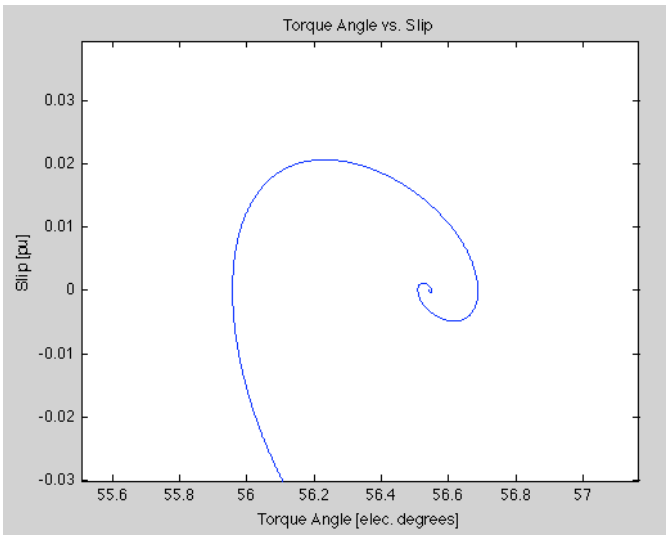

Fig. 8. Inset of pull-in details of Fig. 7.

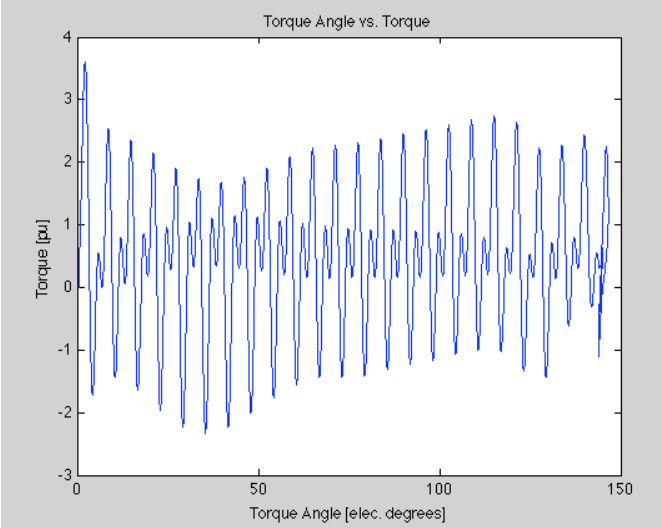

Fig. 9. Nonsalient δ-torque characteristic.

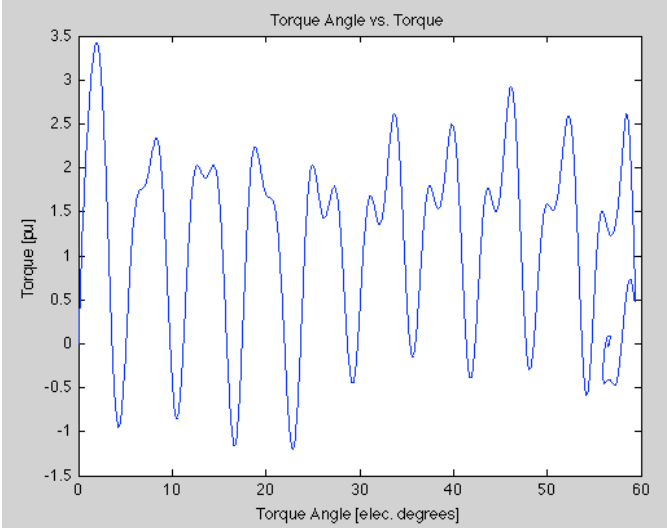

Fig. 11. Salient δ-torque characteristic.

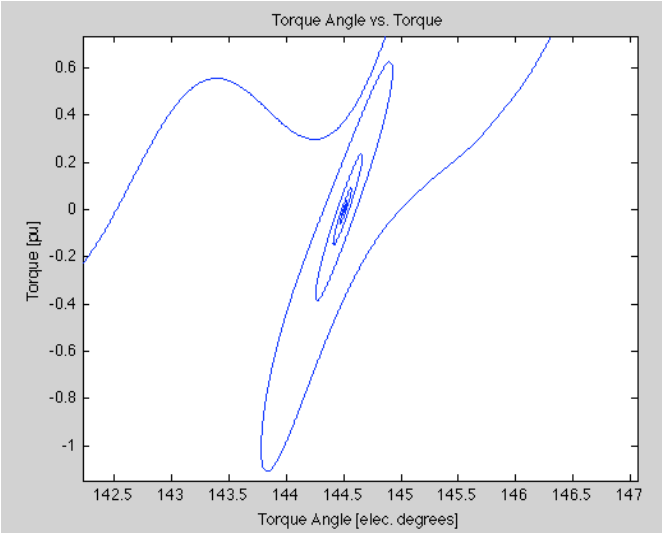

Fig. 10. Inset of pull-in details of Fig. 9.

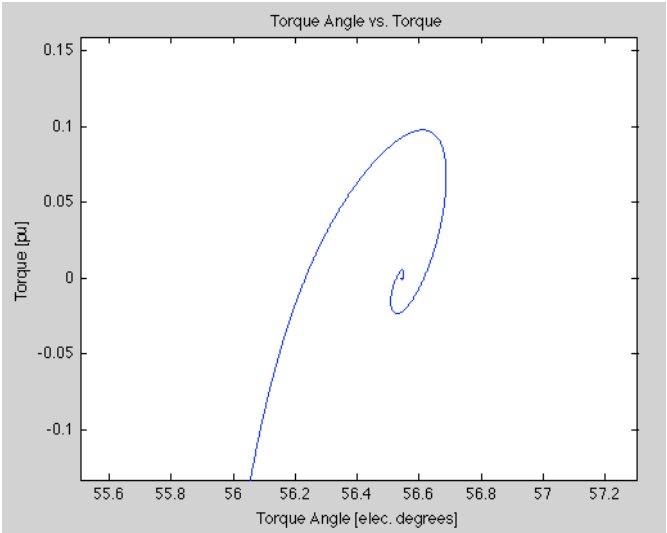

Fig. 12. Inset of pull-in details of Fig. 11.

Figs. 9-12 emphasize the differences in asynchronous starting between the nonsalient and salient LS-PMSMs. The essential details of LS-PMSM asynchronous starting are summed up by the idea of transitioning between different torques. At first, the rotor speed is created through the torque produced by the short-circuited rotor cage. This cage torque creates the average torque needed to spin the rotor up to the synchronous speed; but, at the synchronous speed, this cage torque becomes zero. Therefore, a transition period needs to occur. This transition occurs in the vicinity of the point of synchronization. The machine speed, at first, is induced by the cage torque up until synchronism, and then, at this point and afterward, is sustained by the torque of the permanent magnets and, in the case the salient machine, the reluctance torque. It is this saliency of the machine that adds an additional layer of dynamics to the asynchronous starting performance of the LS-PMSM.

Finally, table 2 summarizes the analysis of the steady state variables for the two machines. The essential difference is the torque angle. This angle is much larger for the nonsalient machine because it lacks reluctance torque. These values were in line with the values obtained in the simulation analysis.

TABLE 2
STEADY-STATE ANALYSIS SUMMARY

Steady State Analysis		
Quantity	Magnitude	Angle
Voltage	1	δ
Back EMF	0.8	0
Current	0.2871	δ
Impedance	0.08805	75.127°

Machine Type	δ
Non-salient	144.5071°
Salient	56.5422°

V. Summary and Conclusions

The LS-PMSM offers advantages over other machines due to higher power factor and efficiency. Although, steady state analysis of this machine needs only basic phasor analysis tools, the dynamics of the asynchronous start-up of this machine proves less trivial. This paper presented the derivation of the ac machine equations – derived from Park's equations for salient pole synchronous machines – for the LS-PMSM, the simulation of this machine in both salient and nonsalient cases, and the presentation of the results of these simulations, specifically focused on performance during the pull-in of the machine into synchronism.

The interaction of the LS-PMSM's multiple torques gave this machine very interesting characteristics. Three torque quantities exist in the general case: 1) cage torque, 2) magnet torque, and 3) reluctance torque. For the salient pole machine, a difference in saliency induces the reluctance torque. This torque gives the salient pole machine characteristics that differ from the nonsalient case. Specifically, the machine will pull-into synchronism quicker, the torque angle will be smaller at this point, and the machine will exhibit fewer oscillations before synchronization occurs.

Further investigations of this topic of saliency could include varying the range of the saliency ratio. This analysis may show additional limitations or opportunities for the use of the saliency of the machine to a machine designer's advantage.

Appendix

The simulation software used for this analysis was Simulink, which is a part of a basic MATLAB software package.

Acknowledgement

I would like to acknowledge the work of Professor Thomas Jahns in acquiring and posting literature related to line-start permanent magnet synchronous motors from IEEE Transactions on Power Apparatus and Systems to the ECE 711 class website. Also, I would like to acknowledge my WEMPEC officemates (Engineering Hall, Room 1535) for supplying a source of caffeinated drinks (i.e. coffee) and taking time out of their day for me to bounce ideas/problems off of – much thanks!

References

[1] Novotny, D. W., Lipo, T. A., "Vector Control and Dynamics of AC Drives," Oxford University Press. 1996.

[2] Honsinger, V. B., "Permanent Magnet Machines: Asynchronous Operation," IEEE Transactions on Power Apparatus and Systems, Vol. PAS-99, No. 4. July/Aug 1980.

[3] Miller, T. J. E., "Synchronization of Line-Start Permanent-Magnet AC Motors," IEEE Transactions on Power Apparatus and Systems, Vol. PAS-103, No. 7. July 1984.